This is a pre-print of an article published in *CIRP Annals Manufacturing Technology*.
The final authenticated version is available online at: https://doi.org/10.1016/j.cirp.2019.04.048

Maximum length scale requirement in a topology optimisation method based on NURBS hyper-surfaces

Giulio Costa, Marco Montemurro*, Jérôme Pailhès, Nicolas Perry*

Arts et Métiers ParisTech Université de Bordeaux, CNRS, Bordeaux INP, I2M Bordeaux UMR 5295, F-33405 Talence, France
**Corresponding authors, marco.montemurro@ensam.eu (Marco Montemurro), nicolas.perry@ensam.eu (Nicolas Perry)*

Abstract
This paper deals with a new method for handling manufacturing and geometrical requirements in the framework of a general Topology Optimisation (TO) strategy. In particular, the maximum length scale constraint (MLSC) implementation is addressed in order to obtain multiple load paths or to locally limit the size of the component. The classic formulation of the MLSC is revisited in the framework of a density-based TO algorithm wherein the pseudo-density field is represented through a NURBS hyper-surface. The NURBS hyper-surface properties are exploited to effectively formulate the MLSC. The effectiveness of the proposed approach is proven on a meaningful 3D benchmark.

Keywords
Topology Optimisation, Geometric Modelling, Computer Aided Design

1. Introduction

Integrating technological and geometrical requirements in Topology Optimisation (TO) is basic to achieve optimised as well as manufacturable configurations [1]. In the framework of the emerging Additive Manufacturing (AM) technologies, this work deals with the integration of the maximum length scale constraint (MLSC) in the design process. The MLSC provides a limitation on the maximum allowable thickness of topological features. Particularly, this requirement is implemented into a TO algorithm making use of NURBS entities to describe the topology.

An intuitive way to define the MLSC has been suggested by Guest in [2] for 2D structures: the thickness of the material phase evaluated around each mesh element must be lower than a given maximum length scale. An exhaustive explanation about the implementation of the MLSC by making use of both projection methods and aggregation techniques is given in [2]. More recent approaches have been proposed in [3]. Firstly, the technique used in [4] has been generalised and the maximum member size is controlled through a low-pass filter in the frequency domain *via* a Fast Fourier Transform. However, setting the design parameters in the frequency domain does not allow the designer to effectively handle the optimisation. Secondly, the concept of mathematical morphology is used to formulate a suitable MLSC but the provided solutions can exhibit disjoint zones of material phase, which are meaningless from a physical viewpoint. Nevertheless, the interest of integrating the MLSC in TO analyses goes beyond the control of the size of structural elements and it originates from design needs. As remarked in [1,3], the MLSC induces multiple load paths in optimised configurations. This fact has been confirmed in [5], wherein a simplified damage model is included in a density-based TO method: final topologies meet fail-safe engineering requirements. Moreover, as it usually happens when dealing with density-based TO analyses, results evaluated before and after the CAD reconstruction phase are not consistent. In the case of the MLSC, the imposed maximum size condition is not met on the final, reassembled geometry.

To overcome the aforementioned shortcomings, the aim of this work is to generalise the implementation of the MLSC to the 3D case in the framework of the NURBS-based TO algorithm presented in [6,7]. Particularly, some of the NURBS hyper-surfaces properties can be suitably combined with well-established methods in order to effectively integrate the MSLC in the problem formulation.

The paper is outlined as follows. The theoretical background is briefly described in section 2. The NURBS-based approach for 3D TO problems is presented in section 3. The formulation of the MLSC is provided in section 4. Results are shown on a meaningful 3D benchmark in section 5. Finally, section 6 ends the paper with some conclusions and perspectives.

2. Tools and Methods

2.1. The NURBS hyper-surfaces theory

The fundamentals of NURBS hyper-surfaces are briefly recalled here below by using the notation of [8]. A NURBS hyper-surface is a polynomial-based function, defined over a *parametric space* (domain), taking values in the *NURBS space* (codomain). Therefore, if N is the dimension of the *parametric space* and M is the dimension of the *NURBS space*, a NURBS entity is defined as $\boldsymbol{H}$: $\mathbb{R}^N \rightarrow \mathbb{R}^M$. The mathematical formula of a generic NURBS hyper-surface is

$$\boldsymbol{H}(u_1, \dots, u_N) = \sum_{i_1=0}^{n_1} \dots \sum_{i_N}^{n_N} R_{i_1,\dots,i_N}(u_1, \dots, u_N)\, \boldsymbol{P}_{i_1,\dots,i_N}, \qquad (1)$$

where $R_{i_1,\dots,i_N}(u_1, \dots, u_N)$ are the piecewise rational basis functions, which are related to the standard NURBS blending functions $N_{i_k,p_k}(u_k)$, $k = 1, \dots, N$ by means of the relationship

$$R_{i_1,\dots,i_N}(u_1, \dots, u_N) = \frac{\omega_{i_1,\dots,i_N} \prod_{k=1}^{N} N_{i_k,p_k}(u_k)}{\sum_{j_1=0}^{n_1} \dots \sum_{j_N}^{n_N} \left[\omega_{j_1,\dots,j_N} \prod_{k=1}^{N} N_{j_k,p_k}(u_k)\right]}. \qquad (2)$$

In Eqs. (1) and (2) , $\boldsymbol{H}(u_1, \dots, u_N)$ is a M-dimension vector-valued rational function, $(u_1, \dots, u_N)$ are scalar dimensionless parameters defined in the interval [0,1], whilst $\boldsymbol{P}_{i_1,\dots,i_N}$ are the so called *control points*, which strongly affect the NURBS shape. The j-th control point coordinate $(X^{(j)}_{i_1,\dots,i_N})$ is stored in the array $\boldsymbol{X}^{(j)}$, whose dimension is $(n_1 + 1) \times \dots \times (n_N + 1)$. For instance, $\boldsymbol{P}_{i_1,i_2} = \{X^{(1)}_{i_1,i_2}, X^{(2)}_{i_1,i_2}, X^{(3)}_{i_1,i_2}\}$ in the case of NURBS surfaces and each coordinate is arranged in a matrix defined in $\mathbb{R}^{(n_1+1)\times(n_2+1)}$. The control points layout is referred as control *hyper-net*. A suitable scalar quantity $\omega_{i_1,\dots,i_N}$ (called *weight*) is related to the respective control point $\boldsymbol{P}_{i_1,\dots,i_N}$. The higher the weight $\omega_{i_1,\dots,i_N}$ value, the more the NURBS entity is attracted towards the control point $\boldsymbol{P}_{i_1,\dots,i_N}$. The blending function of degree p_k related to the parametric direction u_k can be defined in a recursive way as

$$N_{i_k,0} = \begin{cases} 1, & \text{if } U^{(k)}_{i_k} \leq u_k < U^{(k)}_{i_k+1}, \\ 0, & \text{otherwise,} \end{cases} \qquad (3)$$

$$N_{i_k,q}(u_k) = \frac{u_k - U_{i_k}^{(k)}}{U_{i_k+q}^{(k)} - U_{i_k}^{(k)}} N_{i_k,q-1}(u_k) + \frac{U_{i_k+q+1}^{(k)} - u_k}{U_{i_k+q+1}^{(k)} - U_{i_k+1}^{(k)}} N_{i_k+1,q-1}(u_k), \quad q = 1, \dots, p_k,$$

where each constitutive function is defined on the related knot vector

$$\boldsymbol{U}^{(k)} = \{\underbrace{0, \dots, 0}_{p_k+1}, U_{p_k+1}^{(k)}, \dots, U_{m_k-p_k-1}^{(k)}, \underbrace{1, \dots, 1}_{p_k+1}\}, \tag{4}$$

whose size is $m_k + 1$, with $m_k = n_k + p_k + 1$. Each knot vector $\boldsymbol{U}^{(k)}$ is a non-decreasing sequence of real numbers that can be interpreted as a discrete collection of values of the related dimensionless parameter u_k.

NURBS entities are characterised by some interesting properties (the interested reader is addressed to [8] for further details). Here, just the *local support property* is recalled since it is basic for the NURBS-based TO method [6,7,9]: each control point $\boldsymbol{P}_{i_1,\dots,i_N}$ (and the related weight $\omega_{i_1,\dots,i_N}$) affects only a precise zone of the *parametric space* that is precisely referred as a *local support* or *influence zone* ($S_{i_1,\dots,i_N}$), namely

$$S_{i_1,\dots,i_N} = \left[U_{i_1}^{(1)}, U_{i_1+p_1+1}^{(1)}\right[\times \dots \times \left[U_{i_N}^{(N)}, U_{i_N+p_N+1}^{(N)}\right[. \tag{5}$$

2.2. The SIMP Method - Solid Isotropic Material with Penalisation

The classic SIMP method is described here below in the case of 3D TO problems. Consider the compact Euclidean space $D = \{\boldsymbol{x} = \{x_1, x_2, x_3\}^T \in \mathbb{R}^3 : x_j \in [0, a_j]\}$, $j = 1,2,3$, in a Cartesian orthogonal frame $O(x_1, x_2, x_3)$: a_j is a reference length of the domain defined along x_j. For the sake of clarity, the mathematical formulation is here limited to the problem of minimising the compliance of a structure, subject to an equality constraint on the volume [10]. In this framework, the aim of TO is to search for the distribution of a given isotropic "heterogeneous material" (i.e. the definition of void and material zones) on the design domain D in order to minimise the virtual work of external loads applied to the structure and, meanwhile, to meet a suitable volume equality constraint. Let $\Omega \subseteq D$ be the *material domain*. In the SIMP approach, Ω is determined by means of a fictitious density function $\rho(\boldsymbol{x}) \in [0,1]$ defined over the whole design domain D. Such a density field is related to the material distribution: $\rho(\boldsymbol{x}) = 0$ means absence of material, whilst $\rho(\boldsymbol{x}) = 1$ implies completely dense base material. The density field affects the stiffness tensor $E_{ijkl}(\boldsymbol{x})$, which is variable over the domain D, according to

$$E_{ijkl}(\rho(\boldsymbol{x})) = \rho(\boldsymbol{x})^{\alpha} E_{ijkl}^0, i, j, k, l = 1,2,3, \tag{6}$$

where E_{ijkl}^0 is the stiffness tensor of the bulk isotropic material and $\alpha \geq 1$ a suitable parameter that aims at penalising all the meaningless densities between 0 and 1. Considering a FE static analysis, the relationship among the vector of applied generalised nodal forces $\boldsymbol{f}$, the vector of degrees of freedom (DOFs) $\boldsymbol{d}$, and the global stiffness matrix of the structure $\mathbf{K}$ is

$$\mathbf{K}\boldsymbol{d} = \left(\sum_{e=1}^{N_e} \rho_e^{\alpha} \mathbf{K}_e\right)\boldsymbol{d} = \boldsymbol{f}, \tag{7}$$

where the global stiffness matrix $\mathbf{K}$ is expressed by interpreting Eq. (6) in the FE framework. In Eq. (7), ρ_e is the fictitious density computed at the centroid of the generic element e, N_e the total number of elements, whilst $\mathbf{K}_e$ is the non-penalised element stiffness matrix expanded over the full set of DOFs of the structure. The compliance of the structure is easily computed as $c = \boldsymbol{d}^T \mathbf{K} \boldsymbol{d}$.

The problem of compliance minimisation subject to an equality constraint on the overall volume can be stated as follows:

$$\min_{\rho_e} c(\rho_e) \quad \text{subject to:} \quad \begin{cases} \mathbf{K}\boldsymbol{d} = \boldsymbol{f}, \\ \frac{V(\rho_e)}{V_{ref}} = \frac{\sum_{e=1}^{N_e} \rho_e V_e}{V_{ref}} = \gamma, \\ \rho_{min} \leq \rho_e \leq 1, e = 1, \dots, N_e. \end{cases} \tag{8}$$

In Eq. (8), V_{ref} is a reference volume, $V(\rho_e)$ is the volume of the material domain Ω, while γ is the assigned volume fraction; V_e is the volume of element e and ρ_{min} represents the density field lower bound, imposed to prevent any singularity for the solution of the equilibrium problem. Of course, the design variables of the TO problem in the classic SIMP framework are the fictitious densities defined at the centroid of each element.

Problem (8) can be solved through a suitable gradient-based algorithm: to this purpose, the explicit expression of derivatives $\frac{\partial c}{\partial \rho_e}$ and $\frac{\partial V}{\partial \rho_e}$ must be retrieved, as discussed in [10].

3. The NURBS-based SIMP Method for 3D Problems

The formulation of the SIMP TO method in the B-Spline framework has been firstly provided in [11] and [12]. The more general formulation in the NURBS framework, by deeply investigating the influence of both discrete and continuous parameters of the NURBS blending functions, is given in [6,7,9].

In the NURBS-based SIMP method, the pseudo-density field is represented through a suitable NURBS entity [6,7,9]. Therefore, NURBS hyper-surface (N = 3, M = 4) is necessary to describe the topology for 3D problems:

$$\rho(u_1, u_2, u_3) = \sum_{i_1=0}^{n_1} \sum_{i_2=0}^{n_2} \sum_{i_3=0}^{n_3} R_{i_1,i_2,i_3}(u_1, u_2, u_3) \hat{\rho}_{i_1,i_2,i_3}. \tag{9}$$

In Eq. (9), $R_{i_1,i_2,i_3}(u_1, u_2, u_3)$ are the NURBS rational basis functions, defined according to Eq. (2). In Eq. (9), $\rho(u_1, u_2, u_3)$ constitutes the fourth coordinate of the array $\boldsymbol{H}$ in Eq. (1). Moreover, the dimensionless parameters are directly related to the Cartesian coordinates through $u_j = \frac{x_j}{a_j}, j = 1, 2, 3$.

The NURBS control points and the related weights are identified as *design variables*. They are arranged in the arrays

$$\boldsymbol{\xi}^{(1)} = \{\hat{\rho}_{0,0,0}, \dots, \hat{\rho}_{n_1,0,0}, \hat{\rho}_{0,1,0}, \dots, \hat{\rho}_{n_1,n_2,0}, \dots, \hat{\rho}_{n_1,n_2,n_3}\}, \tag{10}$$

$$\boldsymbol{\xi}^{(2)} = \{\omega_{0,0,0}, \dots, \omega_{n_1,0,0}, \omega_{0,1,0}, \dots, \omega_{n_1,n_2,0}, \dots, \omega_{n_1,n_2,n_3}\}, \tag{11}$$

both defined in $\mathbb{R}^{n_{tot} \times 1}$, with $n_{tot} = (n_1 + 1)(n_2 + 1)(n_3 + 1)$. In Eqs. (10) and (11), $\hat{\rho}_{i_1,i_2,i_3} \in [\hat{\rho}_{min}, 1]$ and $\omega_{i_1,i_2,i_3} \in [\omega_{min}, \omega_{max}]$ $\forall i_j = 0, \dots, n_j, j = 1, 2, 3$.

The other NURBS parameters can be identified as *design parameters*, i.e. their value is set a priori at the beginning of the TO analysis and it is not optimised. A concise discussion on the effect of these parameters on the optimised topology is given here below. For more details, the interested reader is addressed to [6,7,9].

- *Degrees*: increasing the degree implies broadening the local support size and the effects of this operation are, on the one hand, a smoother boundary for the optimised topology and, on the other hand, a worse convergence towards more efficient configurations.
- *The number of control points*: increasing the control points number implies a smaller local support size. Thus, better performances (in terms of objective function) can be

achieved and thinner topological features are allowed. Of course, the computational burden increases.

- *Knot vectors*: the non-trivial knot vectors components appearing in Eq. (4) are uniformly distributed on the interval [0,1].

The classic TO problem of compliance minimisation subject to an equality constraint on the volume of Eq. (8) changes into

$$\begin{cases} \min\limits_{\boldsymbol{\xi}^{(1)},\boldsymbol{\xi}^{(2)}} \dfrac{c(\rho_e)}{c_{ref}} \\ \text{subject to:} \\ \left(\sum_{e=1}^{N_e} \rho_e^{\alpha} \mathbf{K}_e\right)\boldsymbol{d} = \mathbf{K}\boldsymbol{d} = \boldsymbol{f}, \\ \dfrac{V(\xi^{(1)},\xi^{(2)})}{V_{ref}} = \dfrac{\sum_{e=1}^{N_e} \rho_e V_e}{V_{ref}} = \gamma, \\ \xi_k^{(1)} \in [\hat{\rho}_{min}, 1], \\ \xi_k^{(2)} \in [\omega_{min}, \omega_{max}], \forall k = 1, \dots, n_{tot}. \end{cases} \tag{12}$$

In Eq. (12), ρ_e is the generic element pseudo-density, i.e. $\rho_e = \rho(u_1^e, u_2^e, u_3^e) = \rho(x_1^e/a_1, x_2^e/a_2, x_3^e/a_3)$, where the j-th Cartesian coordinate of the element centroid is referred as x_j^e. The objective function is divided by a reference compliance (c_{ref}) to obtain a dimensionless value. The linear index k of Eq. (12) is related to the triplet (i_1, i_2, i_3) via the following relationship

$$k = i_1 + i_2(n_1 + 1) + i_3(n_1 + 1)(n_2 + 1)+1, \tag{13}$$

that is consistent to the assembly of the arrays $\boldsymbol{\xi}^{(1)}$ and $\boldsymbol{\xi}^{(2)}$ of Eqs. (10)-(11).

The computation of the derivatives of both objective and constraint functions with respect to the design variables are needed in order to efficiently solve problem (12) through a gradient-based method. Let $S_k = S_{i_1,i_2,i_3}$ be the local support of control point $\xi_k^{(1)} = \hat{\rho}_{i_1,i_2,i_3}$ (and of the weight $\xi_k^{(2)} = \omega_{i_1,i_2,i_3}$), defined according to Eq. (5) when $N = 3$. Then, consider a general response G, whose derivatives $\frac{\partial G}{\partial \rho_e}$ are known. The general expressions of the derivatives of G with respect to the NURBS control points and weights read

$$\frac{\partial G}{\partial \xi_k^{(l)}} = \sum_{e \in S_k} \frac{\partial G}{\partial \rho_e} \frac{\partial \rho_e}{\partial \xi_k^{(l)}}, l = 1, 2, \tag{14}$$

where the derivatives $\frac{\partial \rho_e}{\partial \xi_k^{(l)}}$ are straightforward to evaluate thanks to Eq. (9) [6,7].

Some consequences of outstanding importance result from the NURBS-based SIMP approach:

- The number of design variables is unrelated to the number of elements. Accordingly, the final optimised topology will not depend upon the mesh quality and size.
- Each control point (with the related weight) affects only those elements whose centroid falls in the local support S_k. This fact results in the definition of an implicit filter, that is of paramount importance in density-based TO algorithms in order to avoid numerical artefacts (such as the *checkerboard effect*).

For further details and on the NURBS-based SIMP method, the reader is addressed to [6,7,9].

4. Mathematical Formulation of the Maximum Length Scale Constraint (MLSC)

The aim of this section is to formulate a suitable optimisation constraint on the maximum member size of topological features in the form $g_{d_{max}} \leq 0$. Such a constraint should be able to check the whole design domain and to penalise too thick material zones. Here, the formulation proposed in [6] for 2D applications, based on Guest's formulation [2], has been generalised to the 3D case in the framework of the NURBS-based SIMP approach. The intuitive idea is straightforward: for a given structure, a spherical region is drawn around each element centroid. The sphere diameter is equal to the imposed maximum length scale (referred as d_{max} hereafter). Let Δ_e be the spherical region centred at element e. Its volume is $\frac{4}{3}\pi\left(\frac{d_{max}}{2}\right)^3$. Thus, the condition that should be met for each element reads

$$\sum_{i \in \Delta_e} \bar{\rho}_i V_i \leq \frac{4}{3}\pi\left(\frac{d_{max}}{2}\right)^3 (1 - \psi), \forall e = 1, \dots, N_e. \tag{15}$$

In Eq. (15), i is a mute index pointing at those elements whose centroid falls into Δ_e, $\psi \in [0,1]$ is a relaxing parameter, V_i is the volume of element i and $\bar{\rho}_i$ is the projected fictitious density function evaluated at the centroid of element i. Such a projection is performed through the relation

$$\bar{\rho}_i = \rho_i^{\beta}, \tag{16}$$

where $\beta \geq 1$ is a penalisation parameter (its effects are similar to those of the parameter α of the SIMP method, as shown in section 2.2). In other words, it is explicitly asked that the maximum material phase thickness is locally lower or equal to d_{max}. Being impossible to handle the optimisation constraint of Eq. (15) for each element, a suitable aggregation technique is considered. Choosing the maximum value of the left-hand side of Eq. (15) is a smart strategy, preventing compensatory side effects.

Let δ_e be the left term of Eq. (15), i.e.

$$\delta_e = \sum_{i \in \Delta_e} \bar{\rho}_i V_i. \tag{17}$$

In order to consider the maximum operator in a gradient-based algorithm, a smooth approximation should be given. The χ-norm is used here below:

$$\delta_{max} = \left(\sum_{e=1}^{N_e} \delta_e^{\chi}\right)^{\frac{1}{\chi}}. \tag{18}$$

In Eq. (18), χ is a tuning parameter whose value should be high enough. Therefore, the MLSC can be formulated by combining Eq. (15) with Eq. (18) and by reordering terms:

$$g_{d_{max}} = \frac{\left(\sum_{e=1}^{N_e}\left(\sum_{i \in \Delta_e} \rho_i^{\beta} V_i\right)^{\chi}\right)^{\frac{1}{\chi}}}{\frac{4}{3}\pi\left(\frac{d_{max}}{2}\right)^3 (1-\psi)} - 1 \leq 0. \tag{19}$$

The gradient of the MLSC with respect to the optimisation variables (i.e. the NURBS control points and weights) must be computed. The analytical expression of the constraint derivatives is reported here below. For more details about the related mathematical passages to get these results, the reader is addressed to [6,7].

$$\frac{\partial g_{d_{max}}}{\partial \xi_k^{(1)}} = \beta(g_{d_{max}} + 1) \frac{\sum_{e=1}^{N_e}\left(\left(\sum_{i \in \Delta_e} \rho_i^{\beta} V_i\right)^{\chi-1}\left(\sum_{i \in \Delta_e} \rho_i^{\beta-1} V_i R_k^i\right)\right)}{\sum_{e=1}^{N_e}\left(\sum_{i \in \Delta_e} \rho_i^{\beta} V_i\right)^{\chi}}, \tag{20}$$

$$\frac{\partial g_{d_{max}}}{\partial \xi_k^{(2)}} = \frac{\xi_k^{(1)}}{\xi_k^{(2)}} \frac{\partial g_{d_{max}}}{\partial \xi_k^{(1)}} + \frac{\beta(g_{d_{max}}+1)}{\xi_k^{(2)}} \frac{\sum_{e=1}^{N_e}\left(\left(\sum_{i \in \Delta_e} \rho_i^{\beta} V_i\right)^{\chi-1}\left(\sum_{i \in \Delta_e} \rho_i^{\beta-1} V_i R_k^i\right)\right)}{\sum_{e=1}^{N_e}\left(\sum_{i \in \Delta_e} \rho_i^{\beta} V_i\right)^{\chi}}, \tag{21}$$

The MLSC in the form of Eq. (19) presents several advantages. Firstly, the mathematical formulation is simple. Secondly, the

constraint statement is general and applies to whatever kind of element shape (hexahedral, tetrahedral, etc.). Finally, the MLSC can be imposed in particularly hard TO problems as well, which are characterised by a poor convergence rate: this is possible thanks to the "free" parameters β, ψ and χ. In this paper, they have been set as $\beta = 1.1$, $\psi = 0.05$ and $\chi = 15$ and they are not modified during iterations.

5. Results

The effectiveness of the MLSC is proven in this section through the benchmark of Fig. 1. The domain is parametrised with a B-Spline hyper-surface, whose parameters are set as $p_1 = p_2 = p_3 = 2$ and $(n_1 + 1) \times (n_2 + 1) \times (n_3 + 1) = 32 \times 8 \times 12$. The TO analysis is solved through the algorithm SANTO, developed at I2M Laboratory [7,13].

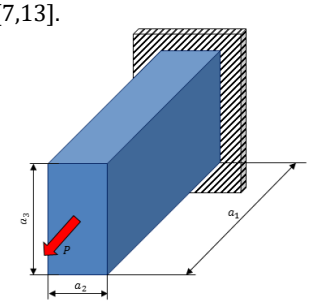

Figure 1 The proposed benchmark: $a_1 = 500$ mm, $a_2 = 100$ mm, $a_3 = 200$ mm, $E = 72$ GPa, $\nu = 0.33$, $60 \times 16 \times 24$ SOLID185 ANSYS elements, $P = 5$ kN.

Firstly, problem (12) is solved without considering the MLSC (c_{ref}=241.42 Nmm, $V_{ref} = 10^7$ mm^3, $\gamma = 0.4$). The result of this optimisation is shown in Fig. 2. The dimensionless compliance of the final configuration is $c/c_{ref} = 0.1422$. Then, problem (12) is enhanced with the MLSC in the form of Eq. (19), wherein the maximum member size is set as $d_{max} = 30$ mm. The solution of problem (12) with the MLSC is shown in Fig. 3 and details about the optimised topology are illustrated in Fig. 4.

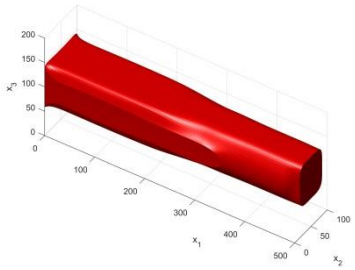

Figure 2 Solution of problem (12).

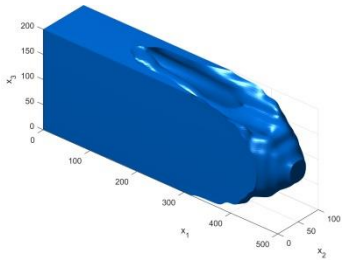

Figure 3 Solution of problem (12) with the MLSC of Eq. (19).

Due to the active constraint on the maximum length scale, the compliance fraction is $c/c_{ref} = 0.2994$. The constraint value is $g_{d_{max}} = 1.601 \times 10^{-6}$: the MLSC is practically met on the whole design domain. It is interesting to remark that the proposed formulation of the MLSC properly works also with a relatively coarse mesh.

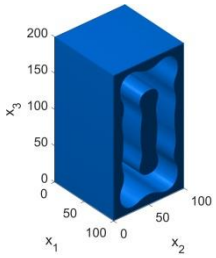

(a) $0 \le x_1 \le 100$.

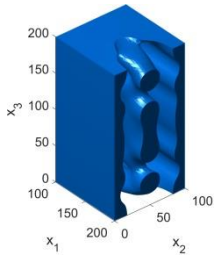

(b) $100 \le x_1 \le 200$.

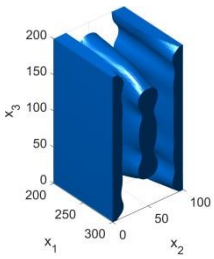

(c) $200 \le x_1 \le 300$.

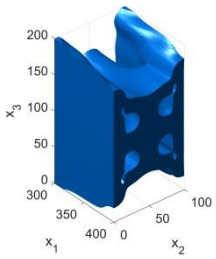

(d) $300 \le x_1 \le 400$.

Figure 4 Details about the solution of problem (12) with MLSC.

6. Conclusions

In this work, the MLSC has been implemented in the framework of the NURBS-based SIMP method for 3D applications. It relies on a suitable extension of the Guest's formulation. Even if the maximum length scale is not completely free from the FE mesh, its effectiveness has been shown in the most general context of 4D NURBS hyper-surfaces. The constraint is strictly met on the reassembled geometry, apart from a limited zone in the neighbourhood of the load application.

Research is ongoing on the formulation of further AM-oriented constraints: the integration (and limitation) of the support material volume and of residual stresses related to the thermodynamic process are challenging perspectives.

References

1. Lazarov BS, Wang F, Sigmund O. Length scale and manufacturability in density-based topology optimization. Arch Appl Mech. 2016 Jan 1;86(1):189–218.
2. Guest JK. Imposing maximum length scale in topology optimization. Struct Multidiscip Optim. 2009 Feb 1;37(5):463–73.
3. Lazarov BS, Wang F. Maximum length scale in density based topology optimization. Comput Methods Appl Mech Eng. 2017 May 1;318:826–44.
4. Kim TS, Kim JE, Jeong JH, Kim YY. Filtering technique to control member size in topology design optimization. KSME Int J. 2004 Feb 1;18(2):253–61.
5. Jansen M, Lombaert G, Schevenels M, Sigmund O. Topology optimization of fail-safe structures using a simplified local damage model. Struct Multidiscip Optim. 2014 Apr;49(4):657–66.
6. Costa G, Montemurro M, Pailhès J. A 2D topology optimisation algorithm in NURBS framework with geometric constraints. Int J Mech Mater Des. 2018 Dec;14(4):669–96.
7. Costa G, Montemurro M, Pailhès J NURBS Hyper-surfaces for 3D Topology Optimisation Problems, Mechanics of Advanced Materials and Structures (2019), in press, URL https://doi.org/10.1080/15376494.2019.1582826;
8. Piegl L, Tiller W. The NURBS Book. Berlin Heidelberg: Springer-Verlag; 1995
9. Costa G, Montemurro M, Pailhes J. A NURBS-based Topology Optimization Method including Additive Manufacturing Constraints. 7th International Conference on Mechanics and Materials in Design. Albufeira/Portugal; 2017.
10. Bendsoe MP, Sigmund O. Topology Optimization: Theory, Methods, and Applications. 2nd ed. Berlin Heidelberg: Springer-Verlag; 2004
11. Qian X. Topology optimization in B-spline space. Comput Methods Appl Mech Eng. 2013 Oct 1;265:15–35.
12. Wang M, Qian X. Efficient Filtering in Topology Optimization via B-Splines1. J Mech Des. 2015 Mar 1;137(3):031402-031402–10.
13. Montemurro M. A contribution to the development of design strategies for the optimisation of lightweight structures, HDR Thesis. 2018;